Atmos. Meas. Tech. Discuss., 6, 10191–10229, 2013
www.atmos-meas-tech-discuss.net/6/10191/2013/
doi:10.5194/amtd-6-10191-2013

Atmospheric Measurement Techniques Discussions

Calibrated high-precision $^{17}O_{excess}$ measurements using laser-current tuned cavity ring-down spectroscopy

E. J. Steig[1,2], V. Gkinis[3,4], A. J. Schauer[1], S. W. Schoenemann[1], K. Samek[1], J. Hoffnagle[5], K. J. Dennis[5], and S. M. Tan[5]

[1]IsoLab, Department of Earth and Space Sciences, University of Washington, Seattle, WA 98195, USA
[2]Quaternary Research Center, University of Washington, Seattle, WA 98195, USA
[3]Centre for Ice and Climate, Niels Bohr Institute, University of Copenhagen, 2100 Copenhagen, Denmark
[4]Institute of Arctic and Alpine Research, University of Colorado, Boulder, CO 80309, USA
[5]Picarro Inc. Santa Clara, CA 95054, USA

Received: 7 October 2013 – Accepted: 15 November 2013 – Published: 29 November 2013

Correspondence to: E. J. Steig (steig@uw.edu)

Published by Copernicus Publications on behalf of the European Geosciences Union.

Abstract

High precision analysis of the $^{17}O/^{16}O$ isotope ratio in water and water vapor is of interest in hydrological, paleoclimate, and atmospheric science applications. Of specific interest is the parameter $^{17}O_{excess}$, a measure of the deviation from a linear relationship between $^{17}O/^{16}O$ and $^{18}O/^{16}O$ ratios. Conventional analyses of $^{17}O_{excess}$ are obtained by fluorination of H_2O to O_2 that is analyzed by dual-inlet isotope ratio mass spectrometry (IRMS). We describe a new laser spectroscopy instrument for high-precision $^{17}O_{excess}$ measurements. The new instrument uses cavity ring-down spectroscopy (CRDS) with laser-current tuning to achieve reduced measurement drift compared with previous-generation instruments. Liquid water and water vapor samples can be analyzed with better than 8 per meg precision for $^{17}O_{excess}$ using integration times of less than 30 min. Calibration with respect to accepted water standards demonstrates that both the precision and the accuracy are competitive with conventional IRMS methods. The new instrument also achieves simultaneous measurements of $\delta^{18}O$, $\delta^{17}O$ and δD with precision < 0.03 ‰, < 0.02 ‰ and < 0.2 ‰, respectively.

1 Introduction

Measurements of the stable isotope ratios of water are ubiquitous in studies of the earth's hydrological cycle and in paleoclimatic applications (Dansgaard, 1964; Dansgaard et al., 1982; Johnsen et al., 1995; Jouzel et al., 2007). Isotopic abundances are reported as deviations of a sample's isotopic ratio relative to that of a reference water, and expressed in the δ notation as:

$$\delta^i = \frac{{}^iR_{\text{sample}}}{{}^iR_{\text{reference}}} - 1 \quad (1)$$

where ${}^2R = \frac{^2H}{^1H}$, ${}^{18}R = \frac{^{18}O}{^{16}O}$ and ${}^{17}R = \frac{^{17}O}{^{16}O}$.

AMTD
6, 10191–10229, 2013

One important innovation was the development by Merlivat and Jouzel (1979) of a theoretical understanding of "deuterium excess":

$$d_{\text{excess}} = \delta\text{D} - 8 \cdot \delta^{18}\text{O} \tag{2}$$

where δD is equivalent to δ^2H. The parameter d_{excess} is commonly used as a measure of kinetic fractionation processes such as the evaporation of water from the ocean surface. For example, d_{excess} variations from ice cores have often been used to infer conditions at the moisture source from which polar precipitation is derived (Johnsen et al., 1989; Petit et al., 1991; Cuffey and Vimeux, 2001; Masson-Delmotte et al., 2005).

The δ^{18}O and δD isotopic ratios can be experimentally determined via a number of isotope ratio mass spectrometry (IRMS) techniques. For δ^{18}O, equilibration with CO_2 has been the standard method for many decades (Cohn and Urey, 1938; McKinney et al., 1950; Epstein, 1953). For δD, reduction of water to H_2 over hot U (Bigeleisen et al., 1952; Vaughn et al., 1998) or Cr (Gehre et al., 1996) has typically been used. Simultaneous determination of δ^{18}O and δD was made possible via the development of continuous-flow mass spectrometric techniques utilizing conversion of water to CO and H_2 in a pyrolysis furnace (Begley and Scrimgeour, 1997; Gehre et al., 2004).

A recent innovation is the measurement of the difference between δ^{18}O and δ^{17}O at sufficiently high precision to determine very small deviations from equilibrium. In general, the nuclei mass difference of $+1n^0$ and $+2n^0$ implies that the fractionation factor for δ^{17}O between two different phases will be approximately the square-root of the fractionation factor for δ^{18}O (Urey, 1947; Craig, 1957; Mook, 2000):

$$\frac{^{17}R_s}{^{17}R_r} = \left(\frac{^{18}R_s}{^{18}R_r}\right)^{\lambda} \tag{3}$$

where $\lambda \approx 0.5$ and the subscripts s and r refer to different phases or samples. For thermodynamic equilibrium, the value of λ is given theoretically by the ratio of the partition

AMTD
6, 10191–10229, 2013

functions (Q), which for the oxygen isotope ratios is as follows (Matsuhisa et al., 1978):

$$\lambda = \ln\left(\frac{Q_{17}}{Q_{18}}\right) = \frac{\frac{1}{16} - \frac{1}{17}}{\frac{1}{16} - \frac{1}{18}} = 0.529 \quad (4)$$

By analyzing a set of meteoric waters, Meijer and Li (1998) estimated the value of λ to be 0.528. Barkan and Luz (2005) used careful water equilibrium experiments to verify that the equilibrium value for λ is 0.529, in accordance with Matsuhisa et al. (1978), while Barkan and Luz (2007) showed that λ is 0.518 under purely diffusive (kinetic) conditions, also in good agreement with theory (Young et al., 2002). Thus, the Meijer and Li (1998) value of 0.528 for meteoric waters reflects the combination of equilibrium and diffusive processes in the hydrological cycle.

Based on these observations, Barkan and Luz (2007) defined the $^{17}O_{excess}$ parameter as the deviation from the meteoric water line with slope 0.528 in $\ln(\delta + 1)$ space:

$$^{17}O_{excess} = \ln(\delta^{17}O + 1) - 0.528 \cdot \ln(\delta^{18}O + 1) \quad (5)$$

Like d_{excess}, $^{17}O_{excess}$ is sensitive to kinetic fractionation, but unlike d_{excess}, it is nearly insensitive to temperature and much less sensitive than δD and δ^{18}O to equilibrium fractionation during transport and precipitation. Natural variations of $^{17}O_{excess}$ are orders of magnitude smaller than variations in δ^{18}O and δD and are typically expressed in per meg ($\times 10^{-6}$) rather than ‰ ($\times 10^{-3}$).

The potential of $^{17}O_{excess}$ in hydrological research is significant because it provides independent information that may be used to disentangle the competing effects of fractionation at the source, in transport, and in the formation and deposition of precipitation (Landais et al., 2008; Risi et al., 2010). It also has applications in atmospheric dynamics, because of the importance of supersaturation conditions that, during the formation of cloud ice crystals impart a strong isotope signature to water vapor (e.g., Blossey et al., 2010).

AMTD
6, 10191–10229, 2013

Compared to the routine nature of $\delta^{18}O$ and δD analysis, isotopic ratio measurements of ^{17}O, the second heavy isotope of oxygen in terms of natural abundance, are challenging. The greater abundance of ^{13}C than ^{17}O effectively precludes the measurement of $\delta^{17}O$ in CO_2 equilibrated with water by IRMS at mass/charge ratio (m/z) 45. As a result the measurement of $\delta^{17}O$ requires conversion of water to O_2 rather than equilibration with CO_2 or reduction to CO. Meijer and Li (1998) developed an electrolysis method using $CuSO_4$. More recently, Baker et al. (2002) used a fluorination method to convert water to O_2, which was analyzed by continuous flow IRMS; this approach was updated by Barkan and Luz (2005) for dual-inlet IRMS.

The dual-inlet IRMS method can provide high precision and high accuracy $^{17}O_{excess}$ measurements. However, the technique is time consuming, resulting in significantly lower sample throughput when compared to the standard and relatively routine analysis of $\delta^{18}O$ and δD. The fluorination procedure typically requires 45 min per sample, while the dual-inlet mass spectrometric analysis requires 2–3 h. In practice, multiple samples must be processed because of memory effects in the cobalt-fluoride reagent and other issues that can arise in the vacuum line (e.g. fractionation during gas transfer) (Barkan and Luz, 2005). Moreover, while this method provides the most precise available measurements of $^{17}O_{excess}$, measurements of individual $\delta^{18}O$ ratios by this method are generally less precise than those obtained with more traditional approaches.

In recent years, laser absorption spectroscopy in the near and the mid-infrared regions has increasingly been used for isotope analysis. An overview of experimental schemes for different molecules and isotopologues can be found in Kerstel (2005). In the case of water, laser absorption spectroscopy constitutes an excellent alternative to mass spectrometry. The main advantage is the ability to perform essentially simultaneous measurements of the water isotopologues directly on a water vapor sample. As a result, tedious sample preparation and conversion techniques are not necessary. Commercialization of laser absorption spectrometers has recently allowed measurements of water isotope ratios to be performed with high precision and accuracy, provided that a valid calibration scheme is applied (Brand et al., 2009; Gupta et al., 2009;

AMTD
6, 10191–10229, 2013

Gkinis et al., 2010, 2011; Schmidt et al., 2010; Kurita et al., 2012; Wassenaar et al., 2012).

The measurement of $^{17}O/^{16}O$ ratios should in principle not pose any additional challenges when compared to the measurement of $^{18}O/^{16}O$ and D/H. Provided that the absorption lines of interest are accessible by the laser source with no additional interferences from other molecules, a triple isotope-ratio measurement can be performed, resulting in calibrated values for $\delta^{18}O$, $\delta^{17}O$ and δD. In fact, triple isotope-ratio measurements of water have been presented in the past via the use of various laser sources utilizing different optical and data analysis techniques (Kerstel et al., 1999, 2002, 2006; Van Trigt et al., 2002; Gianfrani et al., 2003; Wu et al., 2010). However, precision has not been sufficient to be useful for applications requiring the detection of the very small natural variations in $^{17}O_{excess}$.

In this work we report on development of a new cavity ring-down laser absorption spectrometer that provides both high-precision and high-accuracy measurements of $^{17}O_{excess}$. This instrument is a custom modification of the Picarro, Inc. water isotopic analyzer, model L2130-*i*, a version of which has recently been made available as model L2140-*i*. Critical innovations include (1) the use of two lasers that measure absorption in two different infrared (IR) wavelength regions and (2) modifications to the spectroscopic measurement technique. We also developed a sample introduction system that permits the continuous introduction of a stable stream of water vapor from a small liquid water sample into the optical cavity. In combination with precise control of the temperature and pressure in the optical cavity of the instrument, data averaging over long integration times results in precision of better than 8 per meg in $^{17}O_{excess}$. This work can also be seen as a demonstration of state-of-the-art performance for laser absorption spectroscopy isotope ratio analysis for all four main isotopologues of water ($H_2^{16}O$, $H_2^{17}O$, $H_2^{18}O$ and HDO). We compare our results with high precision IRMS measurements and discuss the advantages as well as limitations of our approach.

AMTD
6, 10191–10229, 2013

2 Methods

2.1 Reporting of water isotope ratios

Normalization to known standards is critical in the measurement of water isotope ratios. By convention, $\delta^{18}O$ of a sample is relative to $^{18}O/^{16}O$ of VSMOW (Vienna Standard Mean Ocean Water) and normalized to $\delta^{18}O$ of SLAP (Standard Light Antarctic Precipitation). "Measured" δ values with respect to VSMOW are determined from the difference of "raw" values calculated directly from the ratio of measured isotopologue abundances:

$$\delta^{18}O_s^{\text{measured}} = \delta^{18}O_s^{\text{raw}} - \delta^{18}O_{\text{VSMOW}}^{\text{raw}} \tag{6}$$

where the subscript s refers to an arbitrary sample. Normalization to SLAP is by:

$$\delta^{17}O_{s/\text{VSMOW-SLAP}}^{\text{normalized}} = \delta^{18}O_s^{\text{measured}} \frac{\delta^{18}O_{\text{SLAP}}^{\text{assigned}}}{\delta^{18}O_{\text{SLAP}}^{\text{measured}}} \tag{7}$$

where $\delta^{18}O_{\text{SLAP}}^{\text{assigned}} = -55.5‰$ is the value assigned by the International Atomic Energy Agency (Gonfiantini, 1978; Coplen, 1988). δD is normalized in the same manner, using $\delta D_{\text{SLAP}}^{\text{assigned}} = -428‰$. We normalize $\delta^{17}O$ using:

$$\delta^{17}O_{s/\text{VSMOW-SLAP}}^{\text{normalized}} = \delta^{17}O_s^{\text{measured}} \frac{\delta^{17}O_{\text{SLAP}}^{\text{assigned}}}{\delta^{17}O_{\text{SLAP}}^{\text{measured}}} \tag{8}$$

There is no IAEA-defined value for $\delta^{17}O_{\text{SLAP}}^{\text{assigned}}$, but Schoenemann et al. (2013) recommended that it be defined such that SLAP $^{17}O_{\text{excess}}$ is precisely zero. We follow that recommendation here; that is, we define:

$$\delta^{17}O_{\text{SLAP}}^{\text{assigned}} = e^{(0.528 \ln(-55.5\times10^{-3}+1))} - 1 \tag{9}$$

AMTD
6, 10191–10229, 2013

which yields $\delta^{17}O^{assigned}_{SLAP} \approx -29.6986‰$, well within the error of published measurements (Schoenemann et al., 2013; Lin et al., 2010; Barkan and Luz, 2005; Kusakabe and Matsuhisa, 2008).

Throughout this paper, all reported values of $\delta^{18}O$, $\delta^{17}O$, δD and $^{17}O_{excess}$ have been normalized as described above, unless specifically noted otherwise. Subscripts are omitted except where needed for clarity.

2.2 $^{17}O_{excess}$ analysis with mass spectrometry

Isotope-ratio mass spectrometry (IRMS) measurements provide the benchmark for comparison with results from analysis of $^{17}O_{excess}$ by CRDS. We used IRMS to establish accurate measurements of the $^{17}O_{excess}$, of four working laboratory standards and the IAEA reference water GISP, calibrated to VSMOW and SLAP. We also used both IRMS and CRDS measurements to determine the δD and $\delta^{18}O$ of the same standards; $\delta^{17}O$ is calculated from the $^{17}O_{excess}$ and $\delta^{18}O$ data. Table 1 reports the values, updated from those reported in Schoenemann et al. (2013).

We used the method described in Schoenemann et al. (2013) to convert water to O_2 by fluorination, following procedures originally developed by Baker et al. (2002) and Barkan and Luz (2005). Two microliters of water are injected into a nickel column containing CoF_3 heated to 370 °C, converting H_2O to O_2, with HF and CoF_2 as byproducts. The O_2 sample is collected in a stainless steel cold finger containing 5A molecular sieve following Abe (2008). To minimize memory effects, a minimum of 3 injections are made prior to collecting a final sample for measurements.

The O_2 sample is analyzed on a ThermoFinnigan MAT 253 dual-inlet mass spectrometer at mass/charge ratios (m/z) 32, 33, and 34 for $\delta^{18}O$ and $\delta^{17}O$, using O_2 gas as a reference. Each mass spectrometric measurement comprises 90 sample-to-reference comparisons. Precise adjustment of both sample and reference gas signals (10 V ±100 mV) permits long-term averaging with no measurable drift, so that the analytical precision is given by simple counting statistics: $\sigma/\sqrt{90}$, where σ is the

AMTD
6, 10191–10229, 2013

standard deviation of the individual sample/reference comparisons. The resulting precision of repeated measurements of O_2 gas is 0.002 ‰, 0.004 ‰, and 0.0037 ‰ (3.7 per meg) for $\delta^{17}O$, $\delta^{18}O$, and $^{17}O_{excess}$ respectively. Reproducibility of the $\delta^{17}O$ and $\delta^{18}O$ ratios of water samples is, in practice, less precise than these numbers indicate, because fractionation can occur during the fluorination process or during the collection of O_2. However, because this fractionation closely follows the relationship $\ln(\delta^{17}O+1) = 0.528\ln(\delta^{18}O+1)$, the errors largely cancel in the calculation of $^{17}O_{excess}$ (Barkan and Luz, 2005; Schoenemann et al., 2013). External precision of the $^{17}O_{excess}$ of repeated water samples ranges from 4 to 8 per meg (Schoenemann et al., 2013).

2.3 $^{17}O_{excess}$ analysis with cavity ring-down spectroscopy

2.3.1 Instrument design

We use modified versions of a cavity ring-down spectroscopy (CRDS) analyzer designed for $\delta^{18}O$ and δD, commercially available as Model L2130-*i*, manufactured by Picarro, Inc. The L2130-*i* is an update to the water-isotope analyzers originally discussed in Crosson (2008). Its uses an invar (Ni-Fe) optical cavity coupled to a near-infrared laser. Optical resonance is achieved by piezoelectric modifications to the length of the cavity. When the intensity in the cavity reaches a predetermined value, the laser source is turned off and the intensity then decays exponentially. The time constant of this decay is the "ring-down time". The ring-down time depends on the reflectivity of the mirrors, the length of the cavity, the concentration of the gas being measured, and the absorption coefficient which is a function of frequency. The frequency is determined with a wavelength monitor constructed on the principle of a solid etalon (Crosson et al., 2006; Tan, 2008).

Determination of $\delta^{18}O$ and δD ratios on the Model L2130-*i* is obtained by measurements of the amplitude of $H_2^{18}O$ and $H_2^{16}O$ and HDO spectral lines from a laser operating in the area of 7200 cm^{-1} (wavelength ≈ 1400 nm). In a modified version, which

AMTD
6, 10191–10229, 2013

we refer to as the L2130-*i*-C, we added a second laser that provides access to another wavelength region, centered on $\sim 7193\,cm^{-1}$ where there are strong $H_2^{17}O$ and $H_2^{18}O$ absorption lines (Fig. 1). Rapid switching between the two lasers allows measurement of all three isotope ratios essentially simultaneously. About 200–400 ring-down measurements are made per second, and complete spectra covering all four isotopologues are acquired in $\sim 0.8\,s$ intervals.

For isotope measurements with the L2130-*i* or L2130-*i*-C under normal operating conditions, water vapor in a dry air or N_2 carrier gas flows continuously through the cavity to maintain a cavity pressure of 50 ± 0.1 Torr at a temperature of $80 \pm 0.01\,°C$, normally at a concentration of 2×10^4 ppm. The flow rate of $40\,sccm^{-1}$ is maintained by two proportional valves in a feedback loop configuration up- and down-stream of the optical cavity. The spectral peak amplitudes are determined from the least-squares fit of discrete measurements of the absorption (calculated from measurements of the ring-down time) to a model of the continuous absorption spectrum.

The spectroscopic technique utilized for the acquisition and analysis of the spectral region relevant to the measurement of the isotopologues of interest is essentially the same as the one used in the earlier commercially available L2130-*i* analyzer. One of the main features of this technique is that optical resonance is obtained by dithering the length of the cavity. As discussed in Results (Sect. 3), we found that drift on timescales longer than a few minutes limited the achievable precision of $^{17}O_{excess}$ measurements to about 20 per meg; this drift is ascribed largely to small but detectable drift in the wavelength monitor.

To improve measurement precision, we developed an updated version of the L2130-*i*-C, hereafter referred to as model L2140-*i*, which incorporates a different spectroscopic method. In the new method, the length of the optical cavity is kept constant during the acquisition a spectrum. Resonance is obtained by dithering of the laser frequency by means of laser current modulation. In this method, known as "laser-current tuning" the frequency for each ring-down measurement is determined directly from the resonance itself, based on the principle that resonance will occur only at frequencies spaced by

AMTD
6, 10191–10229, 2013

integer multiples of the free spectral range (FSR) of the cavity. The FSR is inversely proportion to the (fixed) cavity length. The FSR under normal operating conditions is $\approx 0.02\,\mathrm{cm}^{-1}$, and varies by no more than $10^{-5}\,\mathrm{cm}^{-1}$ owing to the precisely controlled temperature and pressure conditions. The wavelength monitor is still used for feedback to the laser frequency control electronics, thus allowing for rapid tuning to a frequency near the desired resonance, but the fine frequency spacing for a given narrow spectral region (e.g., that for $H_2^{17}O$) is determined only by the FSR. In this way, each ring-down measurement can be unambiguously assigned to a stable and equidistant frequency axis. Additionally, the new scheme yield higher cavity excitation rates – typically 500 ring-downs per second. Further details on the laser-current tuning method are provided in a US patent application (Hoffnagle et al., 2013).

2.3.2 Integrated absorption

The use of laser-current turning permits greater accuracy in the determination of the width of spectral lines than was achievable with the L2130-*i* or L2130-*i*-C instruments. This allows us, with the L2140-*i*, to use the integrated absorption under the spectral lines, rather than the height of spectral peaks, to determine isotopologue abundances. The integrated absorption is given by:

$$A = u \int_0^\infty \kappa(\nu)\mathrm{d}\nu \tag{10}$$

where $\kappa(\nu,T,P)$ is the monochromatic absorption coefficient ($\mathrm{cm}^2\,\mathrm{molecule}^{-1}$) and u is the number density of absorbers ($\mathrm{molecules\,cm}^{-2}$). The integrated absorption is directly related to the absorption strength, S, via:

$$\kappa(\nu,T,P) = S(\nu,T)\cdot f(\nu,T,P) \tag{11}$$

where f is the line shape function due to Doppler and pressure spectral line broadening, T is temperature and P is pressure. The integral $\int_0^\infty f(\nu,T,P)\mathrm{d}\nu = 1$ and S is

AMTD
6, 10191–10229, 2013

independent of pressure (e.g, Varghese and Hanson, 1984; Rothman et al., 1996). The ratios A_i/A_j for two different absorbing isotopologues i and j – and therefore in principle the isotope ratios (δ^{18}O, δ^{17}O, etc.) – are also independent of pressure. This makes the integrated absorption superior to the spectral peak amplitude used in earlier-generation instruments.

Values of A are obtained by a least-squares fit of the measurements to an empirically-determined spectral model. The spectral model describes the measured absorption as the sum of a baseline and molecular absorption lines. Free parameters in the baseline are an offset, slope and quadatric curvature term. The molecular absorption spectrum is modeled as the superposition of Galatry profiles, which describe the shape function, f, for each spectral line. The Galatry profile, G is given by the real part of the Fourier transform of the correlation function, Φ (Galatry, 1961):

$$G(x,y,z) = \frac{1}{\sqrt{\pi}} \mathbb{R}\left\{ \int_0^\infty \left[\Phi(y,z,\tau) e^{-ix\tau} \mathrm{d}\tau \right] \right\}$$
$$\Phi(y,z,\tau) = \exp\left(-y\tau + \frac{1}{2z^2}\left[1 - z\tau - e^{-z\tau} \right] \right) \quad (12)$$

where x is the frequency separation from the line center normalized by the Doppler width, y and z are collisional broadening and narrowing parameters, respectively, and τ is dimensionless time.

The parameters that determine the shape of the lines are obtained from spectra acquired by operating the analyzer in a fine-scan mode where ring-downs are acquired with a frequency spacing much smaller than the line width and using the wavelength monitor to determine the frequency axis. This determines the relationship between the collisional broadening and narrowing parameters, y and z, and the relationship between y for the "normal" water peak ($H_2^{16}O$) and the values of y for each of the isotopologues. The Doppler width is a known function of temperature (e.g. Galatry, 1961) and is therefore a fixed parameter. This leaves three or four free parameters

AMTD
6, 10191–10229, 2013

needed to describe absorption for unknown samples in each spectral region: one y-parameter and one value for the integrated absorption, A, for each independent isotopologue spectral line of interest (e.g., one each for the $H_2^{18}O$, $H_2^{16}O$ and HDO lines in the 7200 cm^{-1} wavenumber region).

2.3.3 Determination of isotope ratios

For the determination of $\delta^{18}O$ and $\delta^{17}O$, the $^{18}O/^{16}O$ and $^{17}O/^{16}O$ ratios are obtained from the ratios of integrated absorptions of the rare isotopologues on the second laser to the integrated absorption of the common isotopologue on the first laser:

$$^{18}R = \frac{H_2^{18}O(11)}{H_2^{16}O(2)} \quad (13)$$

$$^{17}R = \frac{H_2^{17}O(13)}{H_2^{16}O(2)} \quad (14)$$

where $H_2^{18}O(11)$, $H_2^{16}O(2)$, etc. refer to the absorption lines shown in Fig. 1.

The raw (uncalibrated) $\delta^{18}O$ and $\delta^{17}O$ values are then obtained using the usual definition of δ:

$$\delta^{18}O^{raw} = \frac{^{18}R}{^{18}R_{ref}} - 1 \quad (15)$$

$$\delta^{17}O^{raw} = \frac{^{17}R}{^{17}R_{ref}} - 1 \quad (16)$$

where the value of R_{ref} is an instrument-specific estimate of the ratio of integrated absorption of $H_2^{17}O$ or $H_2^{18}O$ to that of $H_2^{16}O$ for the IAEA water standard, VSMOW.

AMTD
6, 10191–10229, 2013

Values of δD are determined similarly using data from the first laser only:

$$^2R = \frac{\mathrm{HDO}(3)}{\mathrm{H_2}^{16}\mathrm{O}(2)} \quad (17)$$

$$\delta\mathrm{D}^{\mathrm{raw}} = \frac{^2R}{^2R_{\mathrm{ref}}} - 1 \quad (18)$$

2.4 Sample inlet system

We use two different inlet systems for the introduction of water into the CRDS optical cavity. To obtain measurements of the same water sample continuously over several hours, we use a "custom vaporizer". The custom vaporizer comprises a continuous flow inlet system similar to that described by Gkinis et al. (2010, 2011) and used previously for δ^{18}O and δD. In this design, water is pumped continuously through a capillary and into a stainless steel "Tee" heated to 170 °C. In our application, the "pump" is a simple air pressure system, with a double needle that is used to puncture septum-sealed vials; air pressure introduced into the vial through a small steel tube pushes water through a fused-silica capillary and into the heated Tee. Within the Tee, the liquid water is mixed with dry air and exits the Tee as water vapor that is introduced into the CRDS optical cavity through an open split (Fig. 2). Water vapor concentrations as measured by the CRDS analyzer are maintained at a target value (normally 2×10^4 ppm) to within better than ±100 ppm.

For discrete injections of water into the CRDS we use a commercial vaporizer available from Picarro, Inc. as model A0211 and described by Gupta et al. (2009). The vaporizer, operating at 110 °C, mixes dry carrier gas with 1.8 µL of water, which is injected through a septum. The resulting water vapor is introduced into the optical cavity via a three-way valve after a ∼ 60 s equilibration. Analysis of a single injection pulse takes approximately 120 s, excluding injection, vaporizer purging and equilibration time. Automated sampling from 2 mL vials is accomplished with an autosampler

AMTD
6, 10191–10229, 2013

(LEAP Technologies LC PAL). In our experiments, a complete vial analysis consists of ten repeated injections from the same vial, for a total analysis time of about 1200 s.

3 Results

3.1 Measurement precision and drift

We use the custom vaporizer to obtain CRDS analyses of the isotope ratios of the same water over several hours. The Allan variance statistic provides a convenient way to assess the analytical precision and drift for the resulting long integrations. The Allan variance is defined as (Werle, 2011):

$$\sigma^2_{\text{Allan}}(\tau_m) = \frac{1}{2\,\text{m}} \sum_{j=1}^{m} \left(\overline{\delta}_{j+1} - \overline{\delta}_j\right)^2 \tag{19}$$

where τ_m is the integration time and $\overline{\delta}_{j+1}$, $\overline{\delta}_j$ are the mean values (e.g. $\delta = \delta^{18}\text{O}$ or $^{17}\text{O}_{\text{excess}}$) over neighboring time intervals. Here, we use the "Allan deviation" (σ_{Allan}, square root of the Allan variance) which can be interpreted as an estimate of the achievable external precision as a function of integration time.

Figure 3 shows σ_{Allan} for measurements made both with the L2130-*i*-C instrument using peak amplitudes, and with the L2140-*i* instrument using laser-current tuning and the integrated absorption measurement. In both cases, σ_{Allan} values for $^{17}\text{O}_{\text{excess}}$ of < 20 per meg are achieved after integration times of $\approx 5 \times 10^2$ s, and σ_{Allan} values for $\delta^{18}\text{O}$, $\delta^{17}\text{O}$ and δD are below 0.03, 0.03 and 0.04 ‰, respectively. However, these values represent the limits with the L2130-*i*-C; no additional improvements in precision were achieved with longer integrations times, and in general σ_{Allan} begins to rise after $\approx 10^3$ s. In contrast, with the L2140-*i*, σ_{Allan} values for $\delta^{18}\text{O}$ and $\delta^{17}\text{O}$ improve to < 0.015, and σ_{Allan} for $^{17}\text{O}_{\text{excess}}$ is better than 10 per meg after 1200 s (20 min). For

AMTD
6, 10191–10229, 2013

δD, the precision is < 0.07 ‰ at 10^3 s, and remains well below 0.1 ‰ for much longer integrations times (> 10^4 s). Both the measurements with the custom vaporizer, and those with the commercial vaporizer, show that long term drift in $^{17}O_{excess}$ is greatly reduced in the L2140-*i*. Long term drift for $\delta^{18}O$ or $\delta^{17}O$ is also improved, though not eliminated. We discuss the relationship between drift in $\delta^{18}O$, $\delta^{17}O$ and $^{17}O_{excess}$ in Sect. 4.

Repeated measurements of discrete water injections provide another way to assess measurement precision and drift. Results from running the same water from multiple vials (with 10 discrete 1.8 µL injections per vial), yield statistics comparable to those obtained with the custom vaporizer (Fig. 4). Typical injection-to-injection precision is 20 per meg for $^{17}O_{excess}$. Averages over 10 repeated injections from each vial results in a total analysis time per vial of 10^3 s, corresponding to the integration time at which the Allan deviation data (Fig. 3) show $^{17}O_{excess}$ precision reaching < 10 per meg. Vial average reproducibility of $^{17}O_{excess}$ is ≈ 8 per meg. Typical vial-to-vial reproducibility is 0.03 ‰ for $\delta^{18}O$, 0.015 ‰ for $\delta^{17}O$, 0.1 ‰ for δD.

3.2 Concentration sensitivity

Laser spectroscopy instruments used for water isotope measurements exhibit dependence of $\delta^{18}O$ and δD values on the the water vapor concentration (Gkinis et al., 2010), and similar dependence is expected for $\delta^{17}O$ and $^{17}O_{excess}$. This dependence arises primarily from the effect of pressure broadening on peak shape. As noted in Sect. 2.3.2, use of the integrated absorption in place of peak amplitude in the calculation of isotope ratios with the L2140-*i* instrument should theoretically eliminate the water-vapor concentration dependence. We used the custom vaporizer to obtain measurements on the L2140-*i* over a wide range of water vapor concentrations. Figure 5 shows that there is a significant reduction in the sensitivity of isotope ratios to concentration when using the integrated absorption measurement, as expected. For $\delta^{18}O$, sensitivity is reduced from ≈ 0.2 ‰ for a 1000 ppm variation in H_2O vapor concentration – comparable

AMTD
6, 10191–10229, 2013

to that seen in the L2130-*i* and other earlier-generation instruments – to less than 0.04‰/1000 ppm. Sensitivity for $\delta^{17}O$ is comparably reduced, from ≈ 0.4‰ to less than 0.08‰/1000 ppm. Finally, the sensitivity of $^{17}O_{excess}$ to water vapor concentration is reduced from > 250 per meg to less than 30 per meg/1000 ppm. The concentration sensitivity of δD, at about 1‰/1000 ppm, however, is not significantly changed between earlier models and the L2140-*i*.

3.3 Calibration against VSMOW and SLAP

We performed two independent types of calibration experiments with the L2140-*i*. In the first experiment, we analyzed standard waters SLAP2 and VSMOW2, along with reference waters GISP, VW and WW, and used the two-point calibration line defined by Eqs. (7) and (8) to determine the value of the references waters treated as "unknowns". (Note that the $\delta^{18}O$ and $\delta^{17}O$ of VSMOW2 and SLAP2 are indistinguishable from those of VSMOW and SLAP (Lin et al., 2010).) In the second experiment, we analyzed lab standards PW, VW, SW and WW and used the IRMS $\delta^{18}O$ and $\delta^{17}O$ values of PW and VW as calibration points. The resulting calibrated $\delta^{18}O$ and $\delta^{17}O$ values are then used to calculate $^{17}O_{excess}$, using Eq. (5).

In both types of calibration experiments, we used the commercial vaporizer and sets of four or five consecutive 2 mL vials, from which ten 1.8 µL injections were made. Two sets of each type of water were analyzed in each calibration experiment. The uncertainty of the measurements is given by the standard error of the mean values of repeated sets. To reduce the potential for memory effects influencing the results, we exclude data from the first two or three vials in each set of repeated waters.

The results of the calibration experiments are tabulated in Table 2. Figure 6 shows the calibrated mean values and uncertainties in $^{17}O_{excess}$ for the two different types of calibration experiment. The results show that the $^{17}O_{excess}$ values of the "unknowns" in each experiment with the CRDS are indistinguishable from the values previously-determined using IRMS. Note in particular that the CRDS value of the IAEA reference water, GISP (27 ± 4 per meg), calibrated independently, is nearly identical to the IRMS

AMTD
6, 10191–10229, 2013

value of 28 ± 2 per meg (Schoenemann et al., 2013). Further, we find that both KD (Kona Deep), which is a deep ocean water sample, and VW, which is a meteoric water sample from the interior of East Antarctica (VW) have $^{17}O_{excess}$ values indistinguishable from 0. The CRDS data thus provide independent support for defining $^{17}O_{excess}$ of SLAP to equal that of VSMOW (≡ 0) following Schoenemann et al. (2013). The root-mean square difference between all the IRMS and CRDS data in our analyses is < 3 per meg.

4 Discussion

Our results demonstrate that analysis of $^{17}O_{excess}$ using cavity ring-down laser absorption spectroscopy, as implemented in the L2140-*i* instrument, can be competitive with analyses by mass spectrometry. The precision of repeated individual measurements made over ≈ 30 min is better than 8 per meg, similar to the external precision reported for IRMS (e.g., Luz and Barkan, 2010; Schoenemann et al., 2013), and calibrated values of reference waters are indistinguishable between the two methods. Achieving $^{17}O_{excess}$ measurements at the < 10 per meg level with CRDS requires relatively long integration times when compared with the more common $\delta^{18}O$ or δD measurements, which for typical applications require lower precision (≈< 0.1‰ and ≈ 1‰, respectively). Nevertheless, the new method is significantly less time consuming, less labor intensive, and safer than the IRMS method requiring the use of fluorination.

Measurements of $^{17}O_{excess}$ with a laser spectroscopy instrument with a different design (off-axis integrated cavity output spectroscopy, or OA-ICOS) were reported recently by Berman et al. (2013). It is beyond the scope of this paper to compare the ICOS and CRDS methods, but we note that the results reported by Berman et al. (2013) were obtained by frequent calibration of the instrument with standard waters to correct for drift. Measurements of the IAEA reference water GISP reported by Berman et al. (2013), when calibrated to VSMOW and SLAP, are somewhat lower than ours (23 ± 2 per meg, compared with our value of 27 ± 4), but compatible within 2σ of most

AMTD
6, 10191–10229, 2013

reported IRMS values from the literature; the weighted average of previously-reported measurements (IRMS only) was 22 ± 11 per meg Schoenemann et al. (2013). The mean VSMOW-SLAP normalized value for GISP for all recent IRMS and CRDS measurements from four different laboratories is $^{17}O_{excess}$ = 27 ± 3 per meg (Schoenemann et al., 2013; Berman et al., 2013).

High precision $^{17}O_{excess}$ measurements are achieved without drift correction on the L2140-*i*. Indeed, the precision and drift characteristics of the $^{17}O_{excess}$ results are better than would be expected from the simple combination of noise in the $\delta^{18}O$ and $\delta^{17}O$ measurements, both of which show evidence of some drift in their Allan variances (cf. Fig. 3). The relationship between $\delta^{18}O$, $\delta^{17}O$ and $^{17}O_{excess}$ errors can be understood as a combination of correlated and uncorrelated noise contributions (Schoenemann et al., 2013):

$$\sigma_{xs} = (m - 0.528)\sigma_{18} + \nu_{17} \quad (20)$$

where σ_{xs} is the precision of $^{17}O_{excess}$, σ_{xs} is the precision of $\ln(\delta^{18}O+1)$, and ν_{17} is the residual in $\ln(\delta^{17}O + 1)$ from a best-fit line through the data having slope m.

In general, the uncorrelated errors (ν_{17}) are small. At higher frequencies, m tends towards higher values. We find that for the 0.8 s averages of ≈ 400 individual ring-down measurements, the slope is 0.82 ± 0.02, or 1.0 ± 0.1 if a "model 2" regression that accounts for variance in both the $\delta^{18}O$ and $\delta^{17}O$ measurements is used (e.g. York, 1969). A slope of precisely 1.0 would be expected, for example, if all measurement error were due to noise in the $H_2^{16}O$ spectral line, since this measurement is shared equally in the calculation of both $\delta^{18}O$ and $\delta^{17}O$. The noise in the high frequency data is indistinguishable from Gaussian, and is consequently reduced as a function of the square root of the integration time. For longer measurement times (integrations of 10^3 s or longer), m is ≈ 0.5, so that the term $(m - 0.528)\sigma_{18}$ is small. As for IRMS measurements, it is the combination of the very small magnitude of uncorrelated noise, ν_{17}, combined with $m \approx 0.5$, that leads to the very high precision for $^{17}O_{excess}$ measurements, even where the $\delta^{18}O$ and $\delta^{17}O$ measurements are comparatively imprecise.

AMTD
6, 10191–10229, 2013

We note that frequency-dependence of the error slope, m, is not observed in IRMS measurements. As discussed in Schoenemann et al. (2013), in both the H_2O fluorination procedure and in the mass spectrometer source, likely sources of error will involve some combination of diffusive and equilibrium fractionation processes, both of which will lead to values of m close to 0.5 (e.g., Miller, 2002). That the relationship between $\delta^{18}O$ and $\delta^{17}O$ errors in the CRDS also tends towards $m = \approx 0.5$ at longer integration times suggests that low-frequency drift in these measurements is similarly attributable to fractionation effects, rather than, for example, drift in the optical cavity temperature or other aspects of the CRDS instrument itself. Fractionation of the $\delta^{18}O$ and $\delta^{17}O$ values could be associated with diffusion of water vapor, incomplete evaporation, or condensation and re-evaporation during the vaporization process, or possibly in the optical cavity.

These observations suggest that the current practical limit of precision for isotope measurements on the L2140-*i* is set by the sample introduction system, rather than the CRDS analysis itself. As illustrated in Fig. 8, which compares IRMS and CRDS measurements, the magnitudes of the uncorrelated residuals (ν) are very small – similar to those obtained with high-precision IRMS – while the magnitude of σ_{18} is much smaller than that obtained with IRMS measurements of O_2 prepared by fluorination. This was not the case with our original prototype instrument (L2130-*i*-C), for which analyzer noise was dominant even for long integration times (Fig. 8). We note that since the term $(m - 0.528)\sigma_{18}$ is very small, < 1 per meg, for vial-average measurements, changes to the sample introduction system that would significantly improve $^{17}O_{excess}$ precision will be challenging. These comparisons attest to the significant improvement in the spectroscopic measurements achieved in the L2140-*i*, as well as to the stability of the water vapor delivery and minimal amount of fractionation occurring both in the commercial vaporizer and in our custom vaporizer design.

The L2140-*i* should be useful in a variety of applications, such as in the measurement of ambient water vapor concentrations in the atmosphere, currently done with laser spectroscopy instruments for $\delta^{18}O$ and δD (e.g., Noone et al., 2011; Sayres et al.,

AMTD
6, 10191–10229, 2013

2009), or in the high-resolution analysis of ice core samples using in-line continuous melting systems (Gkinis et al., 2011). The low sensitivity to water-vapor concentration achieved with the integrated-absorption measurement would be an advantage in such applications, though we note that there is still some sensitivity that may become important for concentration variability greater than $\approx \pm 100$ ppm. In the current commercial version of the L2140-*i* instrument, a water-concentration correction is available in the instrument software that uses a bilinear relationship of the form:

$$A(1)_{\text{corrected}} = A(1) + a_0 + a_1 A(1) A(2) \quad (21)$$

where $A(1)$ and $A(2)$ refer to the integrated absorption for peaks 1 and 2 (Fig. 1), and a_0 and a_1 are empirically-determined coefficients. The coefficients are determined by varying the water concentration over a large range and then applied to each measurement. A similar correction is applied to $A(3)$, $A(11)$, and $A(13)$. A simple linear correction following instrument-specific empirical measurements such as illustrated in Fig. 5 could be used as an alternative. We note, however, that we have not evaluated the performance of the instrument at low water vapor concentrations (< 5000 ppm).

As an example of an application of the L2140-*i*, we performed a simple experiment in which 42 vials containing identical water, open to the air, were measured sequentially using 10 injections each. Because the vials were open to a relatively low humidity laboratory atmosphere, evaporation of the vials would be expected to raise the $\delta^{18}O$ values through time, and the $^{17}O_{\text{excess}}$ value should decrease; furthermore, the relationship between $\ln(\delta^{17}O + 1)$ and $\ln(\delta^{18}O + 1)$ would be expected to evolve along a slope intermediate between the equilibrium value (0.529) and the value for diffusion into dry air (0.518) (Barkan and Luz, 2007). These features are indeed observed in the experiment: $^{17}O_{\text{excess}}$ decreases by ≈ 90 per meg and evolves along a slope of 0.523 (Fig. 9). The slope of $\ln(\delta^{17}O + 1)/\ln(\delta^{18}O + 1)$ is 0.5232 ± 0.0005, distinguishable at > 99% confidence from the "meteoric water line" slope of 0.528, as measured with reference water samples and IAEA water standards using the same instrument. A simple experiment like this, which was run fully-automated over ≈ 60 h, would take many hours

AMTD
6, 10191–10229, 2013

of sample preparation time, and > 100 h of analysis time using the traditional fluorination and IRMS method. Note also that the progressive lowering of the $^{17}O_{excess}$ value is clearly detectable from vial to vial at the 1–2 per meg level; this would probably not be possible to observe using the IRMS method. We suggest that the laser spectroscopy method for $^{17}O_{excess}$ could be used in a number of hydrological and atmospheric sciences applications that were previously impractical.

5 Conclusions

Cavity ring-down laser spectroscopy (CRDS) is commonly used for measurements of the $^{18}O/^{16}O$ and D/H isotope ratios of water and water vapor, reported as $\delta^{18}O$ and δD deviations from Vienna Standard Mean Ocean Water (VSMOW). We have developed a new CRDS instrument that makes possible the additional measurement of the $^{17}O/^{16}O$ isotope ratio, and of the small deviation between $\ln(\delta^{17}O+1)$ and $0.528\ln(\delta^{18}O+1)$, known as the $^{17}O_{excess}$. The new instrument uses a novel laser-current tuning method and integrated absorption measurements to achieve precision of < 8 per meg for $^{17}O_{excess}$ while simultaneously providing measurements of $\delta^{18}O$, $\delta^{17}O$ and δD with precision competitive with previous-generation instruments. Liquid samples are introduced into the optical cavity using an automated vaporization system that requires no prior sample preparation. Direct analysis of ambient water vapor in air is also possible. Calibration against the IAEA standard waters VSMOW and SLAP yields values for the reference water GISP of 27 ± 4 per meg, indistinguishable from the value of 28 ± 2 obtained by Schoenemann et al. (2013) using isotope ratio mass spectrometry (IRMS). Our results establish CRDS measurements of $^{17}O_{excess}$ as a viable alternative to conventional IRMS methods that require the use of fluorination to convert H_2O samples to O_2 prior to analysis.

AMTD
6, 10191–10229, 2013

Acknowledgements. We thank B. H. Vaughn, B. Vanden Heuvel, J. W. C. White, B. Vinther, G. Hsiao and E. Crosson. This work was supported by the Quaternary Research Center, University of Washington, the Centre for Ice and Climate, University of Copenhagen, and the US National Science Foundation (award number 1341360).

References

Abe, O.: Isotope fractionation of molecular oxygen during adsorption/desorption by molecular sieve zeolite, Rapid Commun. Mass Sp., 22, 2510–2514, 2008. 10198

Baker, L., Franchi, I. A., Maynard, J., Wright, I. P., and Pillinger, C. T.: A technique for the determination of $^{18}O/^{16}O$ and $^{17}O/^{16}O$ isotopic ratios in water from small liquid and solid samples, Anal. Chem., 74, 1665–1673, 2002. 10195, 10198

Barkan, E. and Luz, B.: High precision measurements of $^{17}O/^{16}O$ and $^{18}O/^{16}O$ ratios in H_2O, Rapid Commun. Mass Sp., 19, 3737–3742, 2005. 10194, 10195, 10198, 10199

Barkan, E. and Luz, B.: Diffusivity fractionations of $H_2{}^{16}O/H_2{}^{17}O$ and $H_2{}^{16}O/H_2{}^{18}O$ in air and their implications for isotope hydrology, Rapid Commum. Mass Sp., 21, 2999–3005, 2007. 10194, 10211

Begley, I. S. and Scrimgeour, C. M.: High-precision δ^2H and $\delta^{18}O$ measurement for water and volatile organic compounds by continuous-flow pyrolysis isotope ratio mass spectrometry, Anal. Chem., 69, 1530–1535, 1997. 10193

Berman, E. S. F., Levin, N., Landais, A., Li, S., and Thomas Owano, T.: Measurement of $\delta^{18}O$, $\delta^{17}O$, and ^{17}O-excess in water by off-axis integrated cavity output spectroscopy and isotope ratio mass spectrometry, Anal. Chem., 85, 10392–10398, 2013. 10208, 10209

Bigeleisen, J., Perlman, M. L., and Prosser, H. C.: Conversion Of hydrogenic materials to hydrogen for isotopic analysis, Anal. Chem., 24, 1356–1357, 1952. 10193

Blossey, P. N., Kuang, Z., and Romps, D. M.: Isotopic composition of water in the tropical tropopause layer in cloud-resolving simulations of an idealized tropical circulation, J. Geophys. Res.-Atmos., 115, D24309, doi:10.1029/2010JD014554, 2010. 10194

Brand, W. A., Geilmann, H., Crosson, E. R., and Rella, C. W.: Cavity ring-down spectroscopy versus high-temperature conversion isotope ratio mass spectrometry; a case study on δ^2H and $\delta^{18}O$ of pure water samples and alcohol/water mixtures, Rapid Commun. Mass Sp., 23, 1879–1884, 2009. 10195

AMTD
6, 10191–10229, 2013

Cohn, M. and Urey, H.: Oxygen exchange reactions of organic compounds and water, J. Am. Chem. Soc., 60, 679–687, 1938. 10193
Coplen, T.: Normalization of oxygen and hydrogen isotope data, Chem. Geol., 72, 293–297, 1988. 10197
Craig, H. H.: Isotopic standards for carbon and oxygen and correction factors for mass-spectrometric analysis of carbon dioxide, Geochim. Cosmochim. Ac., 12, 133–149, 1957. 10193
Crosson, E., Fidric, B., Paldus, B., and Tan, S.: Wavelength control for cavity ringdown spectrometer, Patent US7106763 B2, Picarro, Inc., 2006. 10199
Crosson, E. R.: A cavity ring-down analyzer for measuring atmospheric levels of methane, carbon dioxide, and water vapor, Appl. Phys. B, 92, 403–408, 2008. 10199
Cuffey, K. M. and Vimeux, F.: Covariation of carbon dioxide and temperature from the Vostok ice core after deuterium-excess correction, Nature, 412, 523–527, 2001. 10193
Dansgaard, W.: Stable isotopes in precipitation, Tellus, 16, 436–468, 1964. 10192
Dansgaard, W., Clausen, H., Gundestrup, N., Hammer, C., Johnsen, S., Kristinsdottir, P., and Reeh, N.: A new Greenland deep ice core, Science, 218, 1273–1277, 1982. 10192
Epstein, S. and Mayeda, T.: Variations of ^{18}O content of waters from natural sources, Geochim. Cosmochim. Ac., 4, 213–224, 1953. 10193
Galatry, L.: Simultaneous effect of Doppler and foreign gas broadening on spectral lines, Phys. Rev., 122, 1218–1223, 1961. 10202
Gehre, M., Hoefling, R., Kowski, P., and Strauch, G.: Sample preparation device for quantitative hydrogen isotope analysis using chromium metal, Anal. Chem., 68, 4414–4417, 1996. 10193
Gehre, M., Geilmann, H., Richter, J., Werner, R. A., and Brand, W. A.: Continuous flow $^{2}H/^{1}H$ and $^{18}O/^{16}O$ analysis of water samples with dual inlet precision, Rapid Commun. Mass Sp., 18, 2650–2660, 2004. 10193
Gianfrani, L., Gagliardi, G., van Burgel, M., and Kerstel, E. R. T.: Isotope analysis of water by means of near-infrared dual-wavelength diode laser spectroscopy, Opt. Express, 11, 1566–1576, 2003. 10196
Gkinis, V., Popp, T. J., Johnsen, S. J., and Blunier, T.: A continuous stream flash evaporator for the calibration of an IR cavity ring-down spectrometer for the isotopic analysis of water, Isotop. Environ. Health Stud., 46, 463–475, 2010. 10196, 10204, 10206

AMTD
6, 10191–10229, 2013

Gkinis, V., Popp, T. J., Blunier, T., Bigler, M., Schüpbach, S., Kettner, E., and Johnsen, S. J.: Water isotopic ratios from a continuously melted ice core sample, Atmos. Meas. Tech., 4, 2531–2542, doi:10.5194/amt-4-2531-2011, 2011. 10196, 10204, 10211

Gonfiantini, R.: Standards for stable isotope measurements in natural compounds, Nature, 271, 534–536, 1978. 10197

Gonfiantini, R., Stichler, W., and Rozanski, K.: Standards and Intercomparison Materials Distributed by the International Atomic Energy Agency for Stable Isotope Measurements, Vol. 825 of IAEA-TECDOC, 13–29, International Atomic Energy Agency, Vienna, 1995. 10219

Gupta, P., Noone, D., Galewsky, J., Sweeney, C., and Vaughn, B. H.: Demonstration of high-precision continuous measurements of water vapor isotopologues in laboratory and remote field deployments using wavelength-scanned cavity ring-down spectroscopy (WS-CRDS) technology, Rapid Commun. Mass Sp., 23, 2534–2542, 2009. 10195, 10204

Hoffnagle, J. A., Tan, S. M., and Rella, C.: Regular, stable optical frequency scale for cavity enhanced optical spectroscopy, Us patent application 14/037908, filed on 26 September 2013, Picarro, Inc., 2013. 10201

Johnsen, S. J., Dansgaard, W., and White, J. W. C.: The origin of Arctic precipitation under present and glacial conditions, Tellus B, 41, 452–468, 1989. 10193

Johnsen, S. J., Clausen, H. B., Dansgaard, W., Gundestrup, N. S., Hammer, C. U., and Tauber, H.: The Eem stable-isotope record along the GRIP ice core and its interpretation, Quaternary Res., 43, 117–124, 1995. 10192

Jouzel, J., Masson-Delmotte, V., Cattani, O., Dreyfus, G., Falourd, S., Hoffmann, G., Minster, B., Nouet, J., Barnola, J. M., Chappellaz, J., Fischer, H., Gallet, J. C., Johnsen, S., Leuenberger, M., Loulergue, L., Luethi, D., Oerter, H., Parrenin, F., Raisbeck, G., Raynaud, D., Schilt, A., Schwander, J., Selmo, E., Souchez, R., Spahni, R., Stauffer, B., Steffensen, J. P., Stenni, B., Stocker, T. F., Tison, J. L., Werner, M., and Wolff, E. W.: Orbital and millennial Antarctic climate variability over the past 800 000 years, Science, 317, 793–796, 2007. 10192

Kerstel, E. R. T.: Isotope ratio infrared spectrometry, Vol. 1 of Handbook of Stable Isotope Analytical Techniques, 759–787, Elsevier B. V., Amsterdam, 2005. 10195

Kerstel, E. R. T., van Trigt, R., Dam, N., Reuss, J., and Meijer, H. A. J.: Simultaneous determination of the $^{2}H/^{1}H$, $^{17}O/^{16}O$ and $^{18}O/^{16}O$ isotope abundance ratios in water by means of laser spectrometry, Anal. Chem., 71, 5297–5303, 1999. 10196

AMTD
6, 10191–10229, 2013

Kerstel, E. R. T., Gagliardi, G., Gianfrani, L., Meijer, H. A. J., van Trigt, R., and Ramaker, R.: Determination of the $^{2}H/^{1}H$, $^{17}O/^{16}O$, and $^{18}O/^{16}O$ isotope ratios in water by means of tunable diode laser spectroscopy at 1.39 µm, Spectrochim. Ac. A, 58, 2389–2396, 2002. 10196

Kerstel, E. R. T., Iannone, R. Q., Chenevier, M., Kassi, S., Jost, H. J., and Romanini, D.: A water isotope (^{2}H, ^{17}O, ^{18}O) spectrometer based on optical feedback cavity-enhanced absorption for in situ airborne applications, Appl. Phys. B, 85, 397–406, 2006. 10196

Kurita, N., Newman, B. D., Araguas-Araguas, L. J., and Aggarwal, P.: Evaluation of continuous water vapor δD and δ^{18}O measurements by off-axis integrated cavity output spectroscopy, Atmos. Meas. Tech., 5, 2069–2080, doi:10.5194/amt-5-2069-2012, 2012. 10196

Kusakabe, M. and Matsuhisa, Y.: Oxygen three-isotope ratios of silicate reference materials determined by direct comparison with VSMOW-oxygen, Geochem. J., 42, 309–317, 2008. 10198

Landais, A., Barkan, E., and Luz, B.: Record of delta O-18 and O-17-excess in ice from Vostok Antarctica during the last 150 000 years, Geophys. Res. Lett., 35, L02709, doi:10.1029/2007GL032096, 2008. 10194

Lin, Y., Clayton, R. N., and Groening, M.: Calibration of δ^{17}O and δ^{19}O of international measurement standards – VSMOW, VSMOW2, SLAP, and SLAP2, Rapid Comm. Mass Spectr., 24, 773–776, 2010. 10198, 10207

Luz, B. and Barkan, E.: Variations of $^{17}O/^{16}O$ and $^{18}O/^{16}O$ in meteoric waters, Geochim. Cosmochim. Ac., 74, 6276–6286, 2010. 10208

Masson-Delmotte, V., Jouzel, J., Landais, A., Stievenard, M., Johnsen, S. J., White, J. W. C., Werner, M., Sveinbjornsdottir, A., and Fuhrer, K.: GRIP deuterium excess reveals rapid and orbital-scale changes in Greenland moisture origin, Science, 309, 118–121, 2005. 10193

Matsuhisa, Y., Goldsmith, J. R., and Clayton, R. N.: Mechanisms of hydrothermal crystallization of quartz at 250 °C and 15 kbar, Geochim. Cosmochim. Ac., 42, 173–182, 1978. 10194

McKinney, C. R., McCreal, J. M., Epstein, S., Allen, H. A., and Urey, H. C.: Improvements in mass spectrometers for the measurement of small differences in isotope abundance ratios, Rev. Sci. Instrum., 21, 724–730, 1950. 10193

Meijer, H. A. J. and Li, W. J.: The use of electrolysis for accurate δ^{17}O and δ^{18}O isotope measurements in water, Isotop. Environ. Health Stud., 34, 349–369, 1998. 10194, 10195

Merlivat, L. and Jouzel, J.: Global Climatic Interpretation of the Deuterium-Oxygen 18 Relationship for Precipitation, J. Geophys. Res., 84, 5029–5033, 1979. 10193

AMTD
6, 10191–10229, 2013

Miller, M. F.: Isotopic fractionation and the quantification of ^{17}O anomalies in the oxygen three-isotope system: an appraisal and geochemical significance, Geochim. Cosmochim. Ac., 66, 1881–1889, 2002. 10210

Mook, W.: Environmental Isotopes in the Hydrological Cycle: Principles and Applications, Vol. I, IAEA, Unesco and IAEA, 2000. 10193

Noone, D., Galewsky, J., Sharp, Z. D., Worden, J., Barnes, J., Baer, D., Bailey, A., Brown, D. P., Christensen, L., Crosson, E., Dong, F., Hurley, J. V., Johnson, L. R., Strong, M., Toohey, D., Van Pelt, A., and Wright, J. S.: Properties of air mass mixing and humidity in the subtropics from measurements of the D/H isotope ratio of water vapor at the Mauna Loa Observatory, J. Geophys. Res., 116, D22113, doi:10.1029/2011JD015773, 2011. 10210

Petit, J. R., White, J. W. C., Young, N. W., Jouzel, J., and Korotkevich, Y. S.: Deuterium excess in recent Antarctic snow, J. Geophys. Res., 96, 5113–5122, 1991. 10193

Risi, C., Landais, A., Bony, S., Jouzel, J., Masson-Delmotte, V., and Vimeux, F.: Understanding the ^{17}O excess glacial-interglacial variations in Vostok precipitation, J. Geophys. Res., 115, D10112, doi:10.1029/2008JD011535, 2010. 10194

Rothman, L. S., Rinsland, C. P., Goldman, A., Massie, S. T., Edwards, D. P., Flaud, J.-M., Perrin, A., Camy-Peyret, C., Dana, V., Mandin, J.-Y., Schroeder, J., McCann, A., Gamache, R. R., Wattson, R. B., Yoshino, K., Chance, K. V., Jucks, K. W., Brown, L. R., Nemtchinov, V., and Varanasi, P.: The HITRAN spectroscopic database and HAWKS (HITRAN Atmopsheric Workstation): 1996 edition, J. Quant. Spectrosc. Ra., 60, 665–710, 1996. 10202

Sayres, D. S., Moyer, E. J., Hanisco, T. F., St Clair, J. M., Keutsch, F. N., O'Brien, A., Allen, N. T., Lapson, L., Demusz, J. N., Rivero, M., Martin, T., Greenberg, M., Tuozzolo, C., Engel, G. S., Kroll, J. H., Paul, J. B., and Anderson, J. G.: A new cavity based absorption instrument for detection of water isotopologues in the upper troposphere and lower stratosphere, Rev. Sci. Instrum., 80, 044102, doi:10.1063/1.3117349, 2009. 10210

Schmidt, M., Maseyk, K., Lett, C., Biron, P., Richard, P., Bariac, T., and Seibt, U.: Concentration effects on laser-based $\delta^{18}O$ and $\delta^{2}H$ measurements and implications for the calibration of vapour measurements with liquid standards, Rapid Comm. Mass Spectr., 24, 3553–3561, 2010. 10196

Schoenemann, S. W., Schauer, A. J., and Steig, E. J.: Measurement of SLAP and GISP $\delta^{17}O$ and proposed VSMOW-SLAP normalization for $^{17}O_{excess}$, Rapid Commum. Mass Sp., 27, 582–590, doi:10.1002/rcm.6486, 2013. 10197, 10198, 10199, 10208, 10209, 10210, 10212, 10219, 10226

AMTD
6, 10191–10229, 2013

Tan, S. M.: Wavelength measurement method based on combination of two signals in quadrature, Patent US7420686 B2, Picarro, Inc., 2008. 10199
Urey, H. C.: The thermodynamic poperties of isotopic substances, J. Chem. Soc., 562–581, 1947. 10193
Van Trigt, R., Meijer, H. A. J., Sveinbjornsdottir, A. E., Johnson, S. J., and Kerstel, E. R. T.: Measuring stable isotopes of hydrogen and oxygen in ice by means of laser spectrometry: the Bølling transition in the Dye-3 (south Greenland) ice core, Ann. Glaciol., 35, 125–130, 2002. 10196
Varghese, P. L. and Hanson, R. K.: Collisional narrowing effects on spectral lines shapes measured at high resolution, Appl. Optics, 23, 2376–2385, 1984. 10202
Vaughn, B. H., White, J. W. C., Delmotte, M., Trolier, M., Cattani, O., and Stievenard, M.: An automated system for hydrogen isotope analysis of water, Chem. Geol., 152, 309–319, 1998. 10193
Wassenaar, L. I., Ahmad, M., Aggarwal, P., van Duren, M., Poltenstein, L., Araguas, L., and Kurttas, T.: Worldwide proficiency test for routine analysis of δ^2H and δ^{18}O in water by isotope-ratio mass spectrometry and laser absorption spectroscopy, Rapid Commum. Mass Sp., 26, 1641–1648, 2012. 10196
Werle, P.: Accuracy and precision of laser spectrometers for trace gas sensing in the presence of optical fringes and atmospheric turbulence, Appl. Phys. B, 102, 313–329, 2011. 10205
Wu, T., Chen, W. D., Kerstel, E., Fertein, E., Gao, X. M., Koeth, J., Rossner, K., and Bruckner, D.: Kalman filtering real-time measurements of H_2O isotopologue ratios by laser absorption spectroscopy at 2.73 µm, Opt. Lett., 35, 634–636, 2010. 10196
York, D.: Least squares fitting of a straight line with correlated errors, Earth Planet. Sc. Lett., 5, 320–324, 1969. 10209
Young, E. D., Galy, A., and Nagahara, H.: Kinetic and equilibrium mass-dependent isotope fractionation laws in nature and their geochemical and cosmochemical significance, Geochim. Cosmochim. Ac., 66, 1095–1104, 2002. 10194

AMTD
6, 10191–10229, 2013

Table 1. VSMOW-SLAP normalized isotopic ratios of reference waters analyzed at the University of Washington "Δ*IsoLab". $^{17}O_{excess}$ values are from long-term average IRMS measurements, updated from Schoenemann et al. (2013) to reflect the inclusions of additional data. $\delta^{18}O$ and δD values are from long term average laser spectroscopy measurements. $\delta^{17}O$ values are calculated from $^{17}O_{excess}$ and $\delta^{18}O$ (Eq. 5). Precision (±) is the standard error. n = sample size.

	$^{17}O_{excess}$ (per meg)	$\delta^{18}O$ (‰)	$\delta^{17}O$[a] (‰)	δD (‰)	n
GISP[b]	28 ± 2	−24.80 ± 0.02	−13.1337	−189.67 ± 0.20	20
VW	3 ± 3	−56.61 ± 0.02	−30.3142	−438.79 ± 0.35	10
WW	27 ± 2	−33.82 ± 0.03	−17.9700	−268.30 ± 0.31	36
SW	33 ± 2	−10.55 ± 0.02	−5.5568	−75.63 ± 0.17	18
PW	30 ± 2	−6.88 ± 0.02	−3.6140	−42.12 ± 0.18	17
KD[c]	−0.8 ± 4	0.43 ± 0.01	0.2260	1.33 ± 0.13	5

[a] $\delta^{17}O$ calculated from $\delta^{18}O$ and $^{17}O_{excess}$. See Schoenemann et al. (2013).
[b] CIAAW values for GISP are δD = −189.73 ‰ and $\delta^{18}O$ = −24.78 ‰ (Gonfiantini et al., 1995)
[c] Provisional measurement. Long-term average data for KD (Kona Deep) are not yet available.

AMTD
6, 10191–10229, 2013

Table 2. VSMOW-SLAP normalized $^{17}O_{excess}$, $\delta^{18}O$, $\delta^{17}O$ and δD values for reference waters determined by CRDS using (a) IAEA standards VSMOW2 and VSLAP2 as calibration points and (b) using University of Washington standards PW and VW as calibration points. IRMS-measured $^{17}O_{excess}$ values are shown for comparison. Precision (±) is the standard error. n = sample size.

	IRMS	CRDS				
	$^{17}O_{excess}$ per meg	$^{17}O_{excess}$ per meg	$\delta^{18}O$ ‰	$\delta^{17}O$ ‰	δD ‰	n
GISP[a]	28 ± 2	27 ± 4	−24.77 ± 0.02	−13.13 ± 0.01	−190.19 ± 0.14	6
VW[a]	3 ± 3	−3 ± 3	−56.50 ± 0.03	−30.24 ± 0.02	−438.19 ± 0.35	6
WW[a]	27 ± 2	27 ± 4	−33.90 ± 0.03	−18.02 ± 0.02	−268.87 ± 0.40	6
WW[b]	27 ± 2	27 ± 2	−33.98 ± 0.03	−18.06 ± 0.03	−269.29 ± 0.26	6
SW[b]	33 ± 2	34 ± 4	−10.64 ± 0.04	−5.60 ± 0.03	−76.05 ± 0.24	6
KD[a]	−0.8 ± 4	−1.6 ± 3	0.43 ± 0.01	0.23 ± 0.01	1.33 ± 0.13	6
KD[b]	−0.8 ± 4	−1.6 ± 4	0.50 ± 0.03	0.26 ± 0.03	1.71 ± 0.22	6

[a]VSMOW2 and SLAP2 calibration.
[b]PW and VW calibration. Errors take into account uncertainty in calibration points.

AMTD
6, 10191–10229, 2013

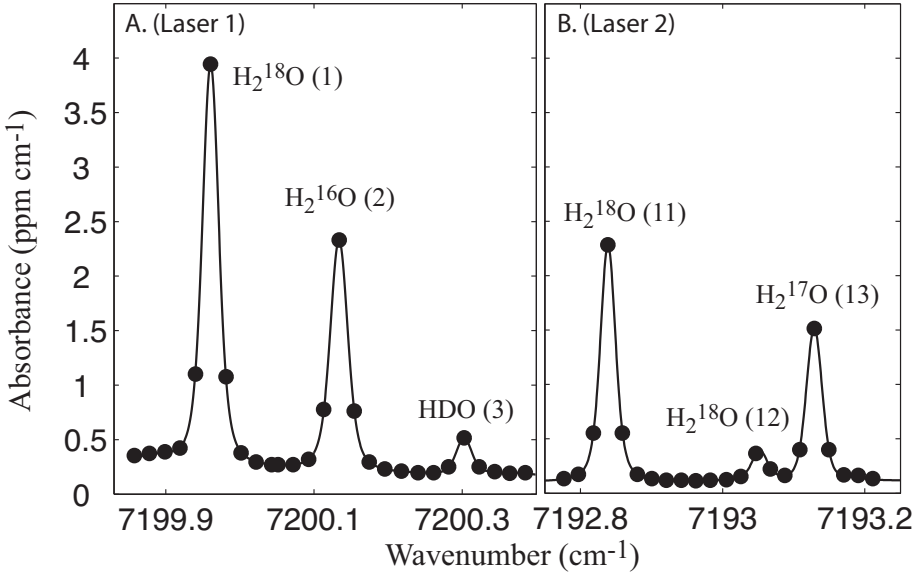

Fig. 1. Measured absorption spectrum for water isotopologues in the two wavenumber regions used by the L2130-*i*-C and L2140-*i* CRDS analyzers. Filled circles: measured absorption for H_2O vapor 20 000 ppm in dry air carrier, 50 Torr cavity pressure. The isotopologue associated with each peak is noted, with nominal peak numbers for reference (1–3 on laser 1, 11–13 on laser 2). Lines: multi-parameter least-squares fit to the data.

AMTD
6, 10191–10229, 2013

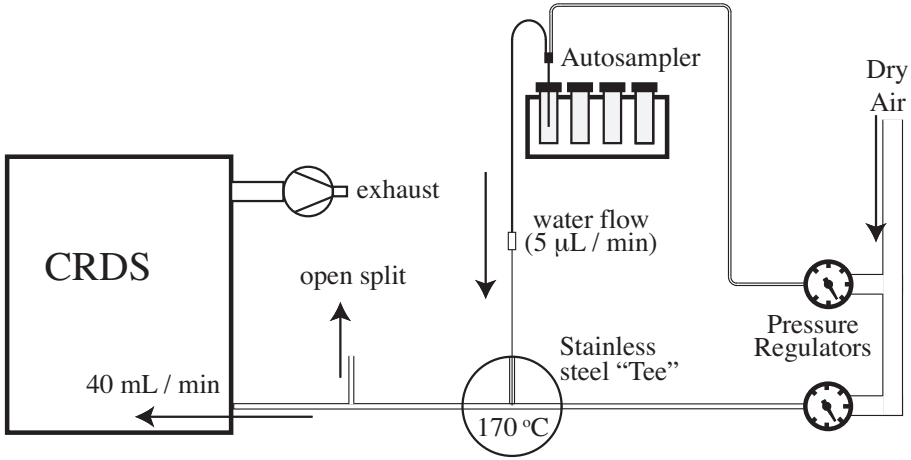

Fig. 2. Schematic of custom vaporizer design used for isotope ratio measurements over long integration times. Double lines denote 1/16 inch and 1/32 inch stainless steel tubing (outside diameter). Single lines denote fused-silica capillary (0.3 mm inside diameter exiting the vials, reduced to 0.1 mm where the capillary enters the vaporizer).

AMTD
6, 10191–10229, 2013

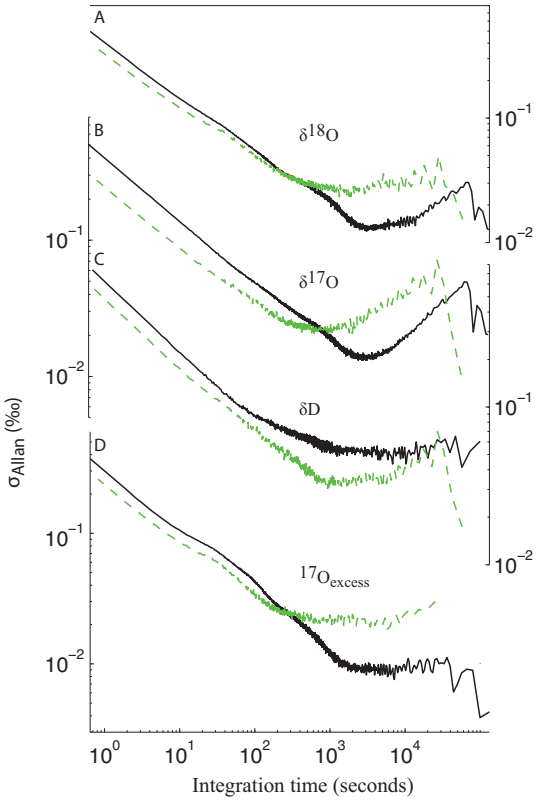

Fig. 3. Comparison of Allan deviations for water isotope ratios with the L2130-*i*-C using conventional wavelength monitor and spectral peak amplitude (green dashed lines), and with the L2140-*i* using laser-current turning and integrated absorption (solid lines). **(A)** δ^{18}O, **(B)** δ^{17}O, **(C)** δD, **(D)** $^{17}O_{excess}$.

AMTD
6, 10191–10229, 2013

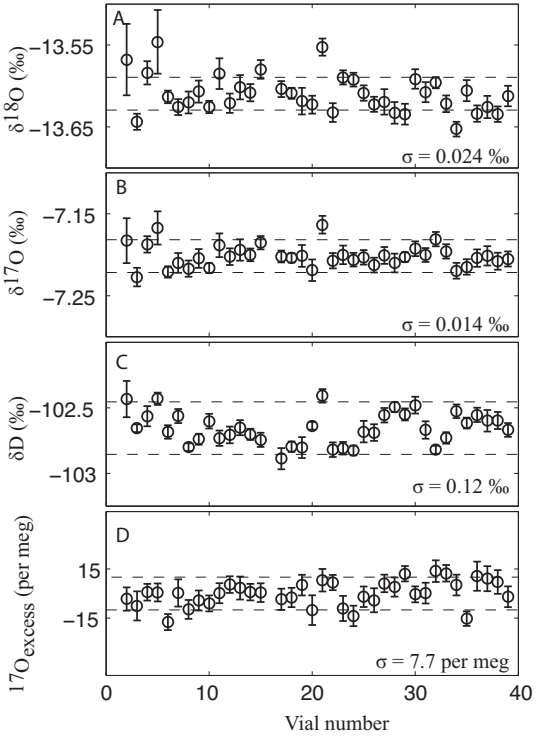

Fig. 4. Isotope ratios from repeated measurements of 2 mL vials of identical water, using integrated absorption on the L2140-*i*. **(A)** δ^{18}O, **(B)** δ^{17}O, **(C)** δD, **(D)** $^{17}O_{excess}$. Each dot represents the average of ten 1.8 µL injections from one vial; the vertical error bars show 1 standard error of the 10 individual injections. The standard deviation of all vial means (σ) is given in each panel. Horizontal dashed lines are shown for reference at ±0.02 ‰ for δ^{18}O and δ^{17}O, at ±0.2 ‰ for δD, and at ±10 per meg for $^{17}O_{excess}$. The experiment shown took about 60 h. No drift corrections or other post-measurement adjustments were made to the raw data.

AMTD
6, 10191–10229, 2013

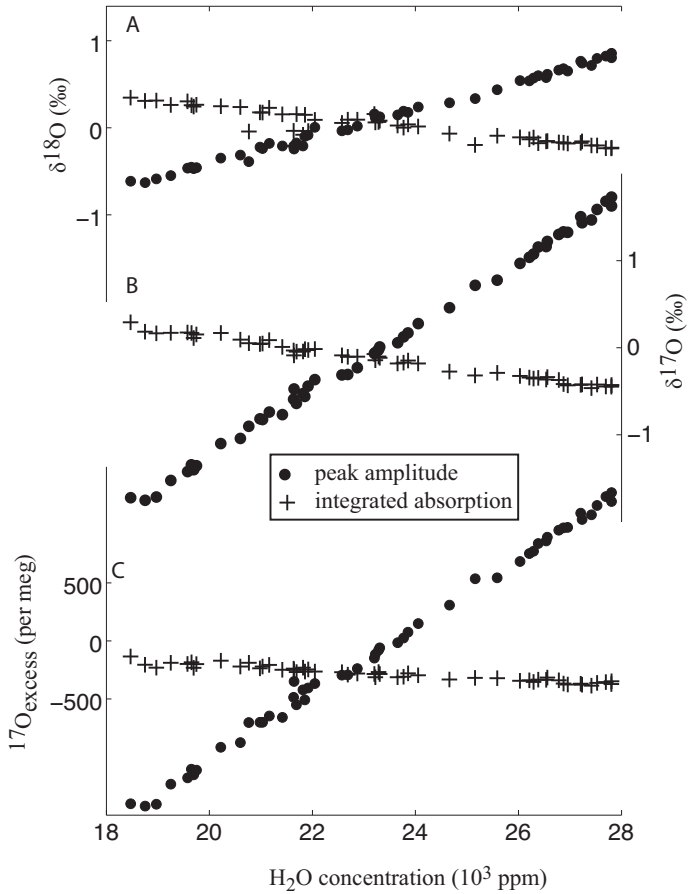

Fig. 5. Comparison of the sensitivity of isotope ratio measurements on the L2140-*i* CRDS analyzer to water vapor concentration, using peak amplitude vs. integrated absorption. **(A)** δ^{18}O, **(B)** δ^{17}O and **(C)** ^{17}O$_{excess}$.

AMTD
6, 10191–10229, 2013

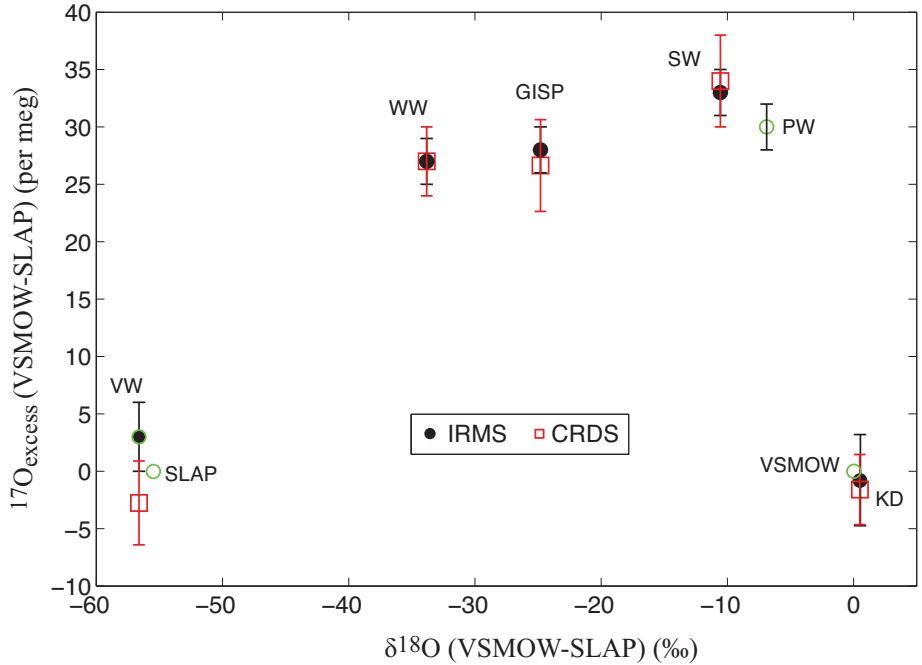

Fig. 6. Comparison of $^{17}O_{excess}$ data from two independent sets of calibrations of reference waters measured by laser spectroscopy on the L2140-*i* (CRDS, open squares) with previously-determined values from mass spectrometry (IRMS, filled circles). $^{17}O_{excess}$ data are plotted vs. $\delta^{18}O$. Error bars (1σ) on the CRDS calibrated values are the standard error of the measurements (see Table 2). Values and error bars (1σ) on the IRMS values are from Table 1, updated from Schoenemann et al. (2013). The calibration points VSMOW, SLAP, PW and VW are shown as open circles for reference.

AMTD
6, 10191–10229, 2013

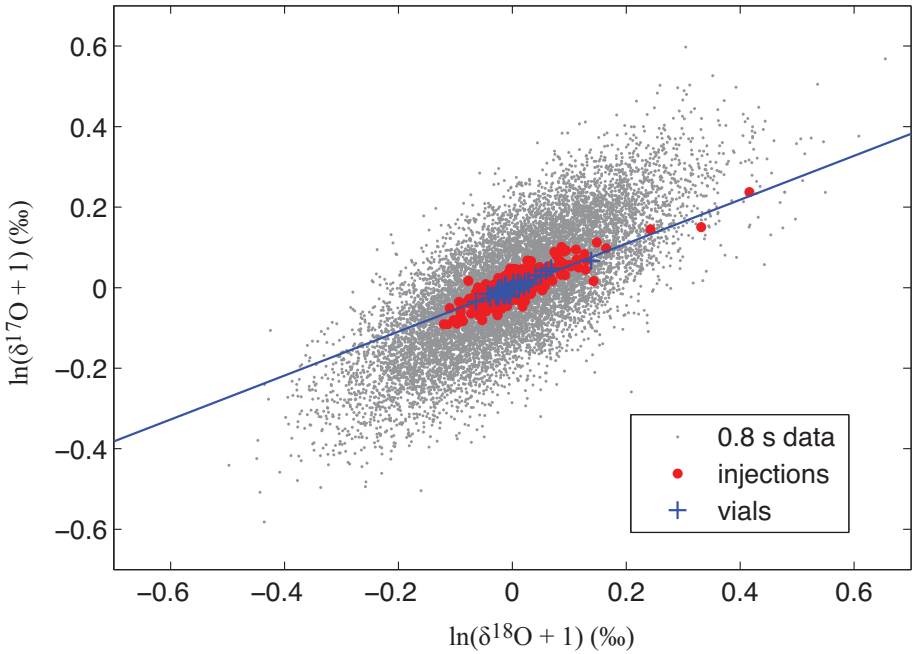

Fig. 7. Relationship between $\ln(\delta^{17}O + 1)$ and $\ln(\delta^{18}O + 1)$ residuals for 40 vials of identical water, each injected 10 times in the L2140-*i* CRDS. Small gray dots show every 100th high-frequency 0.8 *s* measurement, large circles the individual injection means,"+"-signs the vial-mean values. The slopes of the 0.8 *s* and individual injection data are 0.82 ± 0.02 and 0.59 ± 0.02, respectively ($\pm = 2\sigma$). The slope of the vial-mean data is 0.54 ± 0.03, shown by the line.

AMTD
6, 10191–10229, 2013

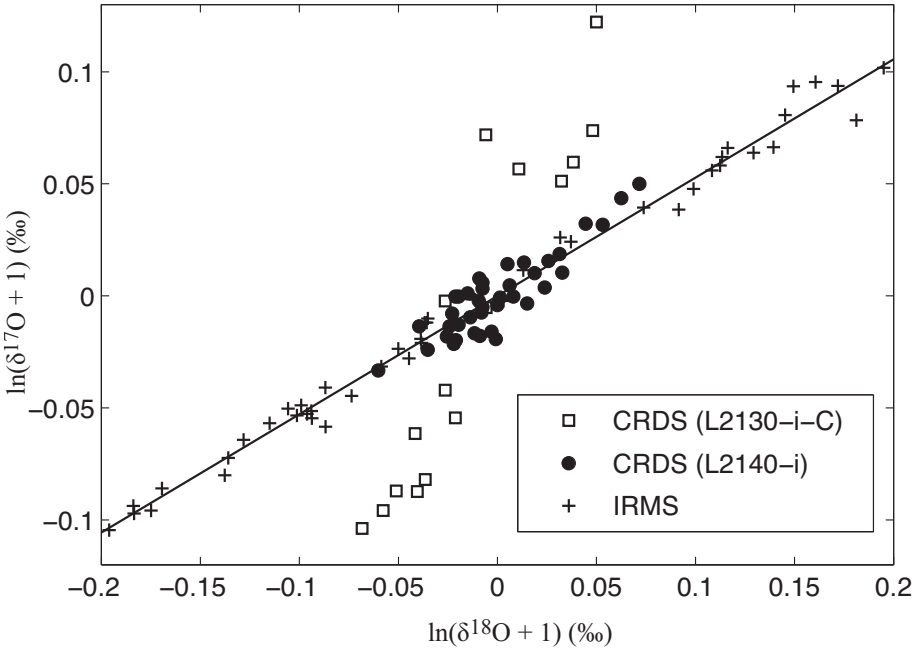

Fig. 8. Comparison of the $\ln(\delta^{17}O + 1)$ vs. $\ln(\delta^{18}O + 1)$ relationship for residuals of measurements of water samples with the L2130-*i*-C and the L2140-*i* CRDS instruments, and with IRMS. The slope of 0.528 that defines $^{17}O_{excess}$ is shown for reference.

AMTD
6, 10191–10229, 2013

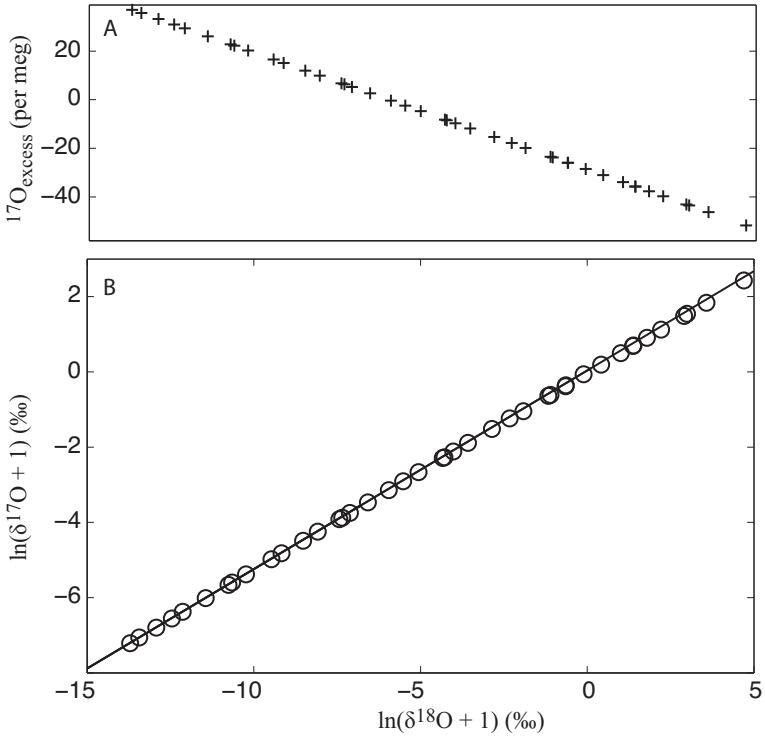

Fig. 9. Results of an evaporation experiment in which 2 mL sample vials are left open to the ambient air and are progressively sampled (ten 1.8µL injections for each vial) over a ≈ 60 h period. **(A)** $^{17}O_{excess}$ vs. $\ln(\delta^{18}O + 1)$, **(B)**, $\ln(\delta^{17}O + 1)$ vs. $\ln(\delta^{18}O + 1)$. Time progress to the right in both panels. Note the gradual deviation of the measurements (open circles) from a slope of 0.528 (line).

AMTD
6, 10191–10229, 2013